2016

Three Dimensional Thermobaric Modeling of A Gas Hydrate System

Amanda Quigley Williams
University of South Carolina

THREE DIMENSIONAL THERMOBARIC MODELING OF A GAS HYDRATE SYSTEM

by

Amanda Quigley Williams

Bachelor of Science
University of South Carolina, 2012

Submitted in Partial Fulfillment of the Requirements

For the Degree of Master of Science in

Geological Sciences

College of Arts and Sciences

University of South Carolina

2016

Accepted by:

Camelia C. Knapp, Director of Thesis

James H. Knapp, Reader

James N. Kellogg, Reader

Leonardo Macelloni, Reader

Lacy Ford, Senior Vice Provost and Dean of Graduate Studies

ACKNOWLEDGEMENTS

First, I would like to thank my family for their support throughout my academic career, especially my husband, Derek Williams, and my parents, Keith and Donna Quigley. I would also like to thank TGS-Nopec and WesternGeco for providing seismic data and the USGS for use of the programming code, HYDROTHERM for heat flow. I thank Dr. Dendy Sloan for providing his hydrate stability code CSMHYD. I thank Doug Cahl for his help with Matlab script development. I would also to thank my committee, Dr. Camelia Knapp, Dr. James Knapp, Dr. James Kellogg, and Dr. Leonardo Macelloni for their support and guidance through both my undergraduate and graduate career. For inspiring my geologic career, I would like to thank Claudia Benitez-Nelson, Robert Thunnell, and Eric Tappa. Lastly, I would like to give a special thank you to the Geophysical Exploration Lab and the Tectonics Lab for their friendship and support, especially Darrell Terry.

ABSTRACT

Seismic imaging is recognized as the most cost effective method for identifying the presence of gas hydrate resources. The base of the gas hydrate stability zone is recognized by the presence of regionally extensive bottom simulating reflectors (BSR). However, in some areas such as the Gulf of Mexico, regionally extensive BSRs are not found. In such cases, an understanding of the thermobaric conditions may be used to determine the location of gas hydrates and the base of the gas hydrate stability zone. The aim of this research is to combine seismic velocity analysis and thermal modeling to predict the base of the hydrate stability zone. As a case study, we apply this modeling to the extensively documented site at Woolsey Mound, MC-118, Gulf of Mexico.

Woolsey Mound, and much of the Gulf of Mexico, has been greatly affected by salt tectonics. Multiple seismic and CHIRP surveys have been collected at Woolsey Mound, but the base of the gas hydrate stability zone has been elusive due to the complexities associated with the presence of salt. The velocity analysis and previous studies on the sedimentary environment were the basis to derive the thermal and salinity conditions. Data from the heat flow survey provide an upper boundary condition at the sea floor in order to create a more accurate thermal model; the velocity model helped accurately place the salt diapir within the mound system. Hydrate phase equilibrium models were used to estimate a thermobaric model for Woolsey Mound. Using two different salinity gradients, the base of the gas hydrate stability zone was found to be located within 70 m of the seafloor with a salt concentration up to 90% at the shallowest point of the salt diapir, and 120 m of the

seafloor with a salt concentration up to standard temperature and pressure conditions of salt (of approximately 56%) at the shallowest point of the salt diapir. This study provides a preliminary look at how the temperature and salinity affect the depth at which gas hydrates are stable over a three dimensional area at Woolsey Mound, MC-118.

TABLE OF CONTENTS

LIST OF FIGURES

List of Abbreviations

BSR ..... Bottom Simulating Reflector

BGHSZ..... Base of the Gas Hydrate Stability Zone

MC-118 ..... Mississippi Canyon Lease Block 118

BOEM .....Bureau of Ocean and Energy Management

GOM-HRC ..... Gulf of Mexico Hydrates Research Consortium

CSMHYD..... Colorado School of Mines Hydrates

CHAPTER 1: THREE DIMENSIONAL THERMOBARIC MODELING OF A GAS HYDRATE SYSTEM, WOOLSEY MOUND, GULF OF MEXICO

1.1 INTRODUCTION

Marine gas hydrates offer significant potential as an alternative fuel because of their extensive distribution in the shallow sediments of the ocean. Gas hydrates are crystalline, ice-like structures that store methane and other greenhouse gases (Collett, 1993) and can be found extensively along the continental shelf of most of the world's oceans, as these regions reach appropriate pressure and temperature conditions necessary for gas hydrate formation. They have been the subject of intensive investigations for more than forty years largely due to their potential as an alternative hydrocarbon fuel. Over the past decade, however, they have begun drawing increasing attention of both the scientific and industrial communities due to three main characteristics, such as (1) potential drilling hazards, (2) considerable fuel resource for the future, and (3) possible role in the global climate change. Among these, the latter has attracted the attention of the scientific community, which has tried to find answers as to whether gas hydrates can drive major changes in the global climate system.

There are three recognized structures for gas hydrate molecules, type I, type, II, and type H (Figure 1.1), all of which consist of a lattice of water molecules surrounding a gas molecule (Buffet, 2000). For each of the three types, different gases are stable within the cage due to the varying shape and size of the vacancies. Type I hydrates are typically

associated with methane storage, due to the smaller size of the two cages of this structure. The gas stored in these molecules is mostly of biogenic origins, produced by organisms in the shallow subsurface. Type II and Type H both consist of larger series of cages, listed in increasing size. This allows for the storage of larger gas molecules and hydrocarbons. Thermogenically sourced gas hydrates are often found in the structure II and H cages, where the guest gas is generated by deeper temperatures typically associated with traditional oil and gas deposits. Due to the scarcity of structure H, Type II is the most common hydrate sought for indication of petroleum resources (Buffet, 2000). Understanding how these structures are affected by their surrounding environment is very useful with respect to their quasi-stable nature and economic or climatic implications.

Gas hydrates are stable at high pressures and at low temperatures and salinities (Kvenvolden, 1993). The depth at which stability occurs is determined by the overlying pressure, the thermal gradient, and the composition of the gas (Sloan, 1990). Pressure and temperature in a structurally undisturbed sedimentary basin largely increase with depth, disregarding the heat associated with the decay of radioactive isotopes. The addition of naturally occurring geologic features such as salt and faults change the thermal environment. These features change the typical temperature profile because of the properties and movements associated with salt, by preferentially channeling heat through the higher conductive salt body. Under the pressure of sediments, salt tends to move as a fluid in order to maintain equilibrium. The movement of large bodies of salt over time, migrating towards equilibrium, disturbs the sediments creating radial faults. The salt, which has a high thermal conductivity, acts as a conduit for temperature as it moves. It is able to maintain heat even with cooler sediments above it and warmer sediments below.

This change in temperature and thermal conductivity associated with the salt, affects the temperature and stability zone of the gas hydrates (Rupel et al., 2005). The salt also changes the free energy of the water molecule in liquid form, which inhibits the gas hydrates ability to form (Buffet, 2000).

In most areas of the world's oceans the presence of gas hydrates are readily identified in seismic sections by the presence of bottom simulating reflectors (BSRs) (Hyndman and Spence, 1992; Singh et al., 1993; Helgerud et al., 1999). In the Gulf of Mexico, gas hydrates are known to exist in abundance but prominent BSRs are not typically present (Shedd et al., 2011). Gas hydrates are affected largely by temperature, salinity, and pressure (Sloan and Koh, 2008). The Gulf of Mexico is noted for its salt diapirs and these diapirs affect both the thermal environment and the salinity, contributing to the lack of extensive BSRs (Liu and Flemings, 2007). The purpose of this research is to understand how the base of the gas hydrate stability zone is affected by changes in temperature and salinity through thermobaric modeling. Thermobaric modeling may prove useful to help better understand the presence and location of potential gas hydrate resources.

The stability zone of gas hydrates normally mimics the shape of the seafloor, as long as pressure and temperature do not change drastically laterally (Shipley et al., 1979). The base of the gas hydrate stability zone (referred to as BGHSZ), is affected by the temperature within the subsurface. The addition of salt introduces a change in temperature and salinity, which changes the depth at which the gas hydrate is stable (Ruppel et al., 2005). Due to the complex tectonic setting of the Gulf of Mexico, typical approaches of determining the BGHSZ have not been reliable. There have been several attempts however to try to define where the gas hydrates are located at MC-118 (Lapham et al. 2008, Macelloni et al., 2012, Simonetti et al., 2013, Macelloni et al., 2015). The study by Simonetti et al. (2013), defined the depth range of the base of the gas hydrate stability

zone around 150 m below sea floor, based on high frequency scattering associated with gas hydrate and a high amplitude bright spot determined to be the free gas/gas hydrate interface, which was found in surface-source deep-receiver single channel seismic. More recently, a 2D thermobaric model has been calculated at Woosley Mound in the Gulf of Mexico which defined a depth range for the BGHSZ from 100 to 230m below sea floor, with depth locations dependent on the proximity to salt and faults (Macelloni et al., 2015). This study extends the thermobaric model over a three dimensional volume to show a map of the BGHSZ as it changes due to temperature and salinity changes, and uses the more recent studies (Simonetti et al., 2013 and Macelloni et al., 2015) as constraints for the model..

1.2. STUDY AREA

The Gulf of Mexico is a region dominated by salt tectonics due to the presence of the Louann salt body (Salvador, 1987). This autochthonous salt body was formed from the evaporation of seawater during the Jurassic, resulting in massive accumulations of salt. The thickness of this salt can reach 4 km and is extensive throughout the Gulf of Mexico basin (Salvador, 1987), extending much of the area from Texas to Florida. The presence of this salt body has greatly impacted the structure and stability of the sediments. As sediments have continued to enter the Gulf of Mexico, pressure from compaction of overlying sediments allowed the lateral movement upward of salt forming diapirs throughout the Gulf of Mexico (Wu et al., 1990).

The upward and lateral intrusion of salt with the sediments disrupts both the structure and conductive properties of the surrounding sediments. Geologic structures formed by salt deformation create effective traps for hydrocarbons, which has helped make the Gulf of Mexico an area rich in this resource. Salt also affects the thermal and salinity properties of the sediments, which determines the stability depth of gas hydrates (Ruppel

et al., 2005). The presence of salt complicates the understanding of where and how much hydrate might be located in the subsurface, but also poses an interesting problem of how the faults associated with the salt affect the gas hydrates (Ruppel et al., 2005). Heat from the salt destabilizes the gas hydrate, and the faults can act as conduits for methane gas to the subsurface (Simonetti et al., 2013). This is a viable migration pathway for the gas upwards, and explains the presence of thriving methane communities and cold seeps at the ocean bottom. Simonetti et al. (2013) showed the presence of high frequency scatter associated with free gas within the subsurface, and concluded that the faults associated with the salt dome were the migration pathways, or source of the gas at the study site. This conclusion means that the source of gas is associated with the salt, but also the salt is the reason these hydrates are not stable, making the study site an ideal area of research for complexities associated with salt affects.

1.2.1 WOOLSEY MOUND AT MC-118

The area of interest is located off the southeastern coast of Louisiana, only 50 km from the delta of the Mississippi River (Figure 1.2). The site Mississippi Canyon lease block 118 (referred to as MC-118), has been allocated as an area for long term research by the Bureau of Ocean Energy Management (BOEM). Located on the upper slope of the continental shelf approximately 900 m below sea level, MC-118 is appropriately located for the presence of methane gas hydrates. Previous research has investigated seafloor activity and processes in the shallow subsurface, including documentation of ocean bottom hydrate and associated carbonate, seafloor morphology and spectral characteristics, benthic and microbial activity, fluid composition and flux at the seafloor, and shallow lithostratigraphy (Lapham et al., 2008; Macelloni et al, 2012; Simonetti et al., 2013).

Three-dimensional seismic data sets have been acquired at MC-118 by TGS Nopec and WesternGeco, in 2000 and 2002 respectively. The seismic data indicates two salt domes located in theMC-118 block, one in the northwest corner and one in the mid-lower portion (Macelloni et al., 2012). The focus of much of the previous research has focus on the salt dome located in the middle portion of the lease block at a site that has been named Woolsey Mound (Figure 1.3), and will be the focus of this study. While a salt dome is clearly found in the seismic data, there is no indication of a regionally extensive bottom simulating reflector (BSR) marking the base of the gas hydrate stability zone. The lack of a BSR in this region is thought to be due to highly complex geologic structures located not only at MC-118, but throughout the Gulf region (Shedd et al., 2011; Macelloni et al., 2012). The presence of salt complicates the salinity of the subsurface, the subsurface sediment structure, and the thermal regime. The high thermal conductivity of the salt, as compared to the lower thermal conductivity of the surrounding sediments, causes heat to be preferentially channeled upwards through the salt dome itself. Seismic analysis has shown the complex nature of the subsurface near the salt dome, and has shown little to no signs of a BSR in the area around the salt (Macelloni et al., 2012). For this reason, an analysis of the geologic and thermal properties must be performed to help estimate the base of the gas hydrate stability zone.

1.3. DATA SETS AND METHODOLGIES

1.3.1 3D SEISMIC SURVEY

TGS Nopec acquired a 3D seismic survey of the MC-118 lease block as a part of a larger survey, in 2000 through GECO. The seismic lines were collected running north to south with a 2ms sample interval and a total record length of 12.288s. Following this

survey, WesternGeco, in 2002, also acquired a 3D seismic survey of the area as part of a larger seismic venture. The lines were recorded running southeast to northwest at a sample interval of 2ms, and a total depth of 12 s. Also provided with the WesternGeco dataset was a velocity analysis of the survey area. The grid resolution was 1000 m by 1000 m, and interpolated later to 500 m by 500 m, with a time interval of every 32 ms. Analysis of the seismic survey indicates a salt dome located in the mid-lower portion of the MC-118 block (Macelloni et al., 2012). The interpreted top of the salt is located in the southwest corner of MC-118 (Figure 1.4). This was provided through extensive seismic picking of the location of the salt in the survey lines, and then saved as a 2D surface in two way travel time. This surface was exported from Kingdom Suite and imported into Matlab. Using the velocity analysis provided by WesternGeco, the salt locations recorded in two way travel time were converted to depth.

1.3.2 HEAT FLOW

In 2012, the Gulf of Mexico Hydrate Research Consortium (GOM-HRC) acquired heat flow measurements through TDI-Brooks, International (Figure 1.5). Fourteen measurements were taken along the sea floor over the salt dome at MC-118, focusing on locations where the major faults associated with the salt dome intersected the seafloor and pockmarks associated with gas venting from the subsurface. These measurements were collected in order to determine a shallow geothermal gradient and measured the heat flow and thermal conductivity at each of the sites (Macelloni et al., 2015). The bottom water temperature indicated by this data collection was an average of 5.6 °C. In order to keep independent data for purposes of validating the results of this study in relation to the Macelloni et al. (2015) study, temperatures were also acquired from the NOAA database

for temperatures in the Gulf of Mexico. The average bottom water temperature was reported to be 5.4 °C over the study site at the average depth of the MC-118 lease block, approximately 900 m.

1.3.3 HYDROTHERM

HYDROTHERM is a finite-element groundwater and heat flow model provided by the USGS. The primary use of HYDROTHERM has been to model fluid flow. However for the purpose of this research, it has been modified to turn off the advection of fluids and produce a steady state model of temperature based on sea floor temperature inputs, and basal heat flow for the Gulf of Mexico. To solve for the temperatures in the basin, the heat transport equation was used.

$$\frac{\partial}{\partial t}[\varphi(\rho_w h_w S_w + \rho_s h_s S_s) + (1-\varphi) * \rho_r h_r] - \nabla \cdot K_a I \nabla T + \nabla \cdot \varphi(S_w \rho_w h_w v_w + S_s \rho_s h_s v_s) - q_{sh} = 0$$

(Equation 1)

where φ is density, h is enthalpy, S is saturation of water, K_a is thermal conductivity, I is the identity matrix, T is temperature, v is interstitial velocity, and q_{sh} is the flow-rate intensity of an enthalpy source, and the subscripts w, s, and r, are water, steam, and rock, respectively. Assuming there is no steam in the system and the water stays in liquid form, all terms with subscripts will become 0, and the saturation of water in the liquid phase (S_w) will be 1, giving:

$$\frac{\partial}{\partial t}[\varphi(\rho_w h_w) + (1-\varphi) * \rho_r h_r] - \nabla \cdot K_a I \nabla T + \nabla \cdot \varphi(\rho_w h_w v_w) - q_{sh} = 0$$

(Equation 2)

If fluid velocity in the pore spaces is assumed to be very slow, or zero ($v_w = 0$) the equation again reduces to:

$$\frac{\partial}{\partial t}[\varphi(\rho_w h_w) + (1-\varphi) * \rho_r h_r] = \nabla \cdot K_a I \nabla T + q_{sh}$$

(Equation 3)

Equation 3 is the equation that is applied by HYDROTHERM to the system by shutting off the terms given the value of zero. The program iterates through time-steps for either a transient or steady state solution. From multiple algorithms available for solving each time step for pressure and temperature, the Newton Raphson method was picked, and the Crank-Nicholson time stepping calculation was used as it is unconditionally stable as compared to both implicit and explicit time stepping (Kipp et al., 2008).

1.3.4 CSMHYD

Developed by Sloan in 1990 and updated in 1998, CSMHYD is a code used to determine where gas hydrates are stable in the subsurface. The code determines the stability of the gas hydrates using a three phase equilibrium analysis of where the hydrates will form based on temperature, pressure, salinity, and gas composition (Sloan, 1990). Much of Sloan's calculations are based on Van der Waals and Platteeuw (1959). Figure 1.1 shows the three structure types for gas hydrates, and the cage sizes associated with each type. Structure I and II clathrate hydrates have two different cage sizes, a small and a large. The two smaller structures are the same size for structure I and II, but the larger cage of Structure II is larger than that of the second, larger cage of structure two. This changes the size of the gas molecule that is able to fit inside of the water cage. When the cages are filled with the appropriately sized molecules and enough of the cages are filled, the gas hydrates are stable (Buffet, 2000). The code determines the phase equilibrium based on gas hydrate composition, which determines the structure type, the temperature, and the effects of any inhibitor (such as salt) in order to produce a pressure that is in equilibrium with these

factors to produce gas hydrate. The resulting pressure and temperature curve is the plot of the phase change between hydrate and free gas, along with water. Further description of the code is reported in Sloan (1998).

1.4. MODELING

1.4.1 VELOCITY MODEL

Through velocity analysis by WesternGeco, stacking velocities were provided along with the seismic data (Figure 1.6). These were converted to interval velocities using Dix Equation,

$$v_{int} = [(t_2 v_{rms2}^2 - t_1 v_{rms1}^2)/(t_2 - t_1)]^{1/2}$$

(Equation 4)

where v_{int} is the interval velocity, t is two-way travel time, and v_{rms} is the stacking velocity or true root mean square velocity. The interval velocity is the velocity over a depth interval and provides information about individual layers. Calculating the interval velocities can be complex because a minor change in the stacking velocity causes an anomalously high interval velocity, as shown in Figure (1.7a). Due to this, the calculated interval velocities were then smoothed (Figure 1.7b). The convolution operator was applied to the box filter, producing a triangle filter. The final velocity model covers an area greater than 57,700 kilometers squared. While it is larger than the region of interest, it allows for the depth conversion of the entire MC-118 lease block.

Figure 1.6, the stacking velocities showed an overall increase in velocity with depth, as was expected. The region where the southwest salt dome is located shows higher velocities than the surrounding sediments, and a velocity high located above the location of the salt dome. There is also a velocity high in the north east portion of the MC-118 lease

block, near the other salt dome located in the region. Figure 1.8, the converted interval velocities, shows a velocity high more than 1000 m/s greater than the sediments above and below located approximately 1,000 m below seafloor in the northeast corner of MC-118 where a salt body is located, and the area where the Woolsey Mound salt dome is located. The velocity at these areas gradually increases to the velocity difference of greater than 1,000 m/s at the locations at the top of the salt domes. There is also a large velocity spike much lower in the section, beginning at 6,000 to 7,000 m below the seafloor, ranging from 1000 – 3000 m/s greater than the surrounding sediment, and the remaining sediment below, reaching a velocity of 8,000 m/s.

1.4.2 SALINITY MODEL

Figure 1.9 shows the top of the salt dome as determined from seismic data. Using the velocity model, the salt tops were converted from two way travel time to depth. A linearly increasing salinity gradient from the seafloor to the top of the salt was generated using two different salt concentration values, and assumed the majority of the salt in the diapir was NaCl. The first salinity gradient ranged from sea floor salinity values to standard temperature pressure values of saturation, or 3.5-56% salt, where standard temperature and pressure are defined as 25 °C and 1 atm. Standard temperature and pressure conditions for the saturation point of salt were chosen for the first model because the saturation point of NaCl changes very little in response to both temperature and pressure. This was set as a minimum for what the concentration of salt had to be at the top of the salt dome, knowing that the true value would likely be much higher. The second gradient included values ranging from sea floor salinity to 90% salt, as the core of a salt dome is documented to be 90-99% salt (US Nuclear Regulatory Commission, 1981). These linearly varying salt

concentrations produced a salinity gradient that changed with respect to how far the top of the salt dome was to the sea floor. The points over the salt dome span 2,900 m by 2,650 m, with 810 different salinity gradients within the area. It is widely understood that salinity does not linearly increase with depth, even in the presence of a salt diapir (Smith et al., 2014; Jamshidzadeh et al., 2015). The salinity gradient is highly affected by the convection of lower density warm waters from deeper sources, and colder, denser waters found in the shallow subsurface. This mixing creates saline rich plumes of water as the salt from the outer region of the salt diapir is dissolved. Most likely, the salt concentrations will increase significantly closer to the salt dome and along the side of the diapir, but will remain relatively low in the shallower sediments (Jamshidzadeh et al., 2015).

1.4.3 THERMAL MODEL

In order to calculate the stability field of the gas hydrates, a model of the thermal environment was constructed based on the sedimentary properties derived through seismic interpretation, lithostratigraphic studies, and heat flow measurements in the shallow seafloor (Macelloni et al, 2012; Simonetti et al., 2013; Macelloni et al., 2015). This is highly dependent on the salt diapirs located at the study site and the contrasting properties of the surrounding sediments. The salt alters the thermal environment due to its relatively high thermal conductivity. In order to model the thermal environment, HYDROTHERM is used. HYDROTHERM can be used as a 1D, 2D, or 3D finite element code. This study interpolates a series of 2D seismic lines to create a 3D volume. To calculate the temperatures in the subsurface, the simplified heat flow equation uses Equation 3. The HYDROTHERM modeling code also allows for pore waters to move through the system, but for the purposes of this research, there was no advection of fluids included, so the

advection term of the heat flow equation is absent. The term remaining on the left hand side of the equation is then the conduction term, which takes into account the density, porosity, and enthalpy of the water and the sedimentary medium. The fluid terms remained the same, and the rock/sediment terms changed based on whether they are salt or sediments. The source and sink terms are represented by q_{sh}, where the source term is an average steady state basal heat flux in the Gulf of Mexico after Husson et al. (2008).

In order to model the temperature, the Woolsey Mound was broken down into 30 different profiles running north to south that were spaced 100 m apart from east to west (Figure 1.10A). Figure 1.10A also shows where the salt has been interpreted in the southern region of MC118, with a color bar corresponding to the depth of the top of the salt. For each profile, a grid was discretized to span 2,700 m, north to south, and 2,400 m depth. The resulting grid was 48 by 48 cells, where the depth covered by each cell was 50 m, and the horizontal distance was 100 m (Figure 1.10B). The location of the salt and the sedimentary properties of the salt and surrounding sediments were then imported into their assigned cell. To simplify the calculations, the surrounding sediments were averaged to one type of sediment that combined the sedimentary properties of the interbedded sand and clays. This provided a model that would calculate the temperatures based on the salt in contrast with the overlying and surrounding sediments.

Figure 1.11 shows a profile view of MC-118, running from south to north, and cutting through the center of the salt dome. The model shows an increase in temperatures in the shallow sediments above the salt dome, as compared to the temperatures further away from the salt dome. Similarly, there was a decrease in temperatures below the salt dome, as compared to the temperatures deeper in the profile away from the salt. A clearly

defined dome shape is present in the temperature profile where the salt is located. This pattern continued through all of the profiles that included that salt dome, with the curvature of the temperatures increasing upward in temperature at shallower depths most prominent at the crest of the salt dome. In the regions where the salt is absent, there are no temperature anomalies and the temperatures increase uniformly with depth, lacking the dome shape change in temperatures. This is indicated by a pseudo-3D temperature plot (Figure 1.12).

1.4.4 THERMOBARIC MODEL

Thermobaric modeling is the pressure and temperature stability modeling between phases in a given system. For gas hydrates, a thermobaric model maps the pressures and temperatures along which the phase change occurs between frozen gas hydrate and free gas. The 1998 version of Sloan's CSYHYD code (Sloan, 1998) was used to calculate the pressures where hydrates are stable based on salt concentrations and the gas composition at a given temperature. The salt concentrations and temperature values are discussed in sections 4.2 and 4.3. The thermobaric model uses the temperature and salinities to calculate a pressure necessary to create a stable environment for gas hydrate formation. Once the pressures are calculated, they can be converted to depth, based on a hydrostatic pore pressure gradient of 0.1 atm/m (Kvenvolden, 1993). Hydrates will form down to the depth where the thermobaric curve for hydrate stability intersects the geothermal gradient. The code itself can only calculate one depth point at a time for a given location, so a Matlab script was written to iteratively run the executable program for increasing depth points at varying locations. The area was defined using the same dimensions as the temperature and salinity models, resulting in a 3,000 m by 2,700 m area covered, with a total of 810 locations to be calculated. Two different models were calculated, with two different salinity

models to show how the salinity of the sediments affects the depth to the BGHSZ. Once the stability pressures were calculated and converted to depth, the thermobaric stability curve and geothermal gradient were graphed in order to find their intersection for the BGHSZ (Figure 1.13). The depth of stability for each of the 810 locations were then plotted in an interpolated mesh grid.

For each of the two models (Figures 1.14 and 1.15), the estimates BGHSZ is located just below the topography, and above the salt diapir. The shape of the stability zones are a thinner dome shape with relationship to the shape of the salt dome. The height of the BGHSZ calculated based on salt concentrations ranging from sea floor levels to STP is 140 m, or 118 m to 158 m below the seafloor. The height of the BGHSZ calculated based on salt concentrations ranging from sea floor levels to 90 weight percent is 119 m, or 67 m to 186 m below the seafloor. The shallowest stability values are at the crest of the salt dome and the deepest stability depths for the two models are at the edges of the salt dome as expected.

1.5 DISCUSSION

1.5.1 MODELING

The Gulf of Mexico is a region known for its gas and oil resources as well as complex salt structures. This has made the mapping of the BGHSZ difficult through typical means which consists of locating a BSR in seismic sections. The salt disrupts the thermal environment by channeling heat through the sediments because of its high thermal conductivity. Salt also inhibits the formation of hydrates by lowering the free energy of water in the liquid phase. By accounting for salinity and temperature changes through thermobaric modeling, the BGHSZ can be estimated, even without an obvious BSR

present. In the presence of salt, we expect to see a thermal high at the shallowest point of the salt dome, and a thinning of the stability zone in the thermobaric model due to the higher temperatures and higher salinity gradient.

Temperature has the greatest effect on gas hydrate stability as it prohibits the water molecule cages from forming. Figure 1.12 shows the temperature distribution at Woolsey Mound. The region where the salt dome is located shows an increase in temperature as compared to the surrounding sediments of the same depth. Similarly, the base of the salt diapir displays lower temperatures than that of the surrounding sediments. As expected, the high thermal conductivity of the salt preferentially funneled heat through the salt system, resulting in the temperature found. In the sediments where there is no salt dome, the temperatures increase at a near linear rate with depth because there is no change in the sediment properties to affect how the heat travels, and any nonlinear temperatures are a result of high heat flow associated with the fault. These affects lessen the further away from the salt diapir the sediments are. This also agrees with the high heat flow values from Macelloni et al. (2015), where the mound system had much higher heat flow values than the sediments located away from the salt dome.

Figures 1.14 and 1.15 show a thin domed layer above the Woolsey Mound salt diapir located below. This is the base of the gas hydrate stability zone. As the salinity and geothermal gradient increase with the shallowing of the salt, the stability zone also shallows. This shallowing is a result of the salinity and temperature inhibiting the formation of the gas hydrates, because the water is unable to freeze and form the ice-like cages of water molecules. Figure 1.14 shows a thicker hydrate stability zone between the topography and the base of the stability zone as compared to Figure 1.15. The higher

salinity gradient used in the calculation of Figure 1.15 causes this shallower stability zone. Based on the properties of salt, which lowers the free energy of liquid water, the shallower result is due to the higher weight percent salt used in Figure 1.15. Figure 1.14 shows a thicker stability zone because the lower salinity gradient has less of an effect on the temperature and hydrate formation. The model displays the properties of hydrates that were expected. An increase in the salinity and temperature blocks hydrate formation, and thins the region where they are stable. Both thermobaric models show this by having a dome shape as the salt diapir crests and also between the two models as the thinner stability zone is associated with a higher salinity gradient (Figure 1.14 and 1.15).

In order to constrain the results of the two 3D thermobaric models (Figure 1.14 and 1.15), the results were compared to the values found in both seismic (Simonetti et al., 2013) and the 2D BGHSZ found using heat flow values along the seafloor (Macelloni et al., 2015). The study by Simonetti et al. (2013) determined a local BGHSZ at the depth range of 150 m below seafloor. This is based on a bright spot found in seismic (Figure 4a) or the interface between the free gas and gas hydrate, and studies of the high frequency scatter found in SSDR data, which has been determined to be gas hydrate. Macelloni et al. (2015) found a depth range for BGHSZ to range from 100m below seafloor to 230m below seafloor in a 2D profile. The study accounted for heat flow at the seafloor and described the change in depth of the BGHSZ as the temperatures changed based on the migration of heat through the faults. Both of the 3D models that calculated the BGHSZ in this study (Figure 1.14 and 1.15) are at the depth range found in both of these studies across Woosley Mound. This places these models at the correct depth range based on both the seismic

interpretation for the BGHSZ (Simonetti et al., 2013) and the BGHSZ calculated using the heat flow study (Macelloni et al., 2015).

1.5.2 FUTURE DIRECTIONS AND CAVEATS

The results of the thermobaric models (Figures 1.14 and 1.15) provide comparable results with the location of the BGHSZ indicated in a two-dimensional model by Macelloni et al. (2015). However, this is only a starting point for a more accurate three-dimensional model mapping the BGHSZ at MC-118. Two detailed models need to be created in order to place a better estimate on where the hydrates at Woolsey Mound are stable. A geologic model and a salinity model used to rerun the thermal and thermobaric models will aid in the accuracy.

As stated in section 4.3, the sediments around the salt diapir were homogenized for the purpose of this study. A geologic model accounting for stratigraphic changes will allow for a more accurate calculation of the salinity and thermal models because the properties of the sediments themselves change how the salinity and temperature are distributed within the subsurface. The current model also disregards the role that faults play in the transport of heat, salinity, and gas. Including the location of the faults in a geologic model to allow for fluid motion in subsequent models would increase the overall accuracy in the estimation of the base of the gas hydrate stability zone.

A salinity model based on the properties determined in the geologic model and calculated using a program to model salt and fluid motion would capture a more realistic salinity gradient that changes with proximity to salt. Faults can act as conduits for the salt, unevenly distributing high salt concentrations to the sediments near the faults, while lack of convection can leave sediments away from the faults and above the salt dome low in salt

concentration. Creating a nonlinear relationship between salt concentrations from the sea floor to the top of the salt dome will greatly enhance the prediction of the BGHSZ.

Creating these two models, and then applying the geologic model to the simplified thermal model will allow for the advection and convection of salt and fluid through the entire system, especially through the faults. The updated salinity and thermal model will change the thermobaric model and is predicted to shallow the stability zone where faults and salt are moving and deepen the stability zone where there is no fluid motion to increase the temperature and salinity. Continuing the research in this direction will improve the accuracy of the thermobaric model and produce a better prediction of the BGHSZ.

1.6. CONCLUSIONS

This study was aimed to produce a 3D estimate of the BGHSZ based on temperature and salinity changes associated with salt diapirs. Thermobaric modeling has been used in the past to determine where the BGHSZ is located in regions where BSRs are not present. Highly dependent on the thermal environment and the salinity gradient, a depth for the hydrate stability zone was determined to exist between 70 and 120 m below the seafloor, at its shallowest point. These estimates corresponded with the nature of gas hydrates, as the hydrates were less likely to form in the areas of higher temperature and salinity. Constraining where these hydrates are stable is important for estimating the volume of gas resources and understanding the destabilization associated with the changes in their environment.

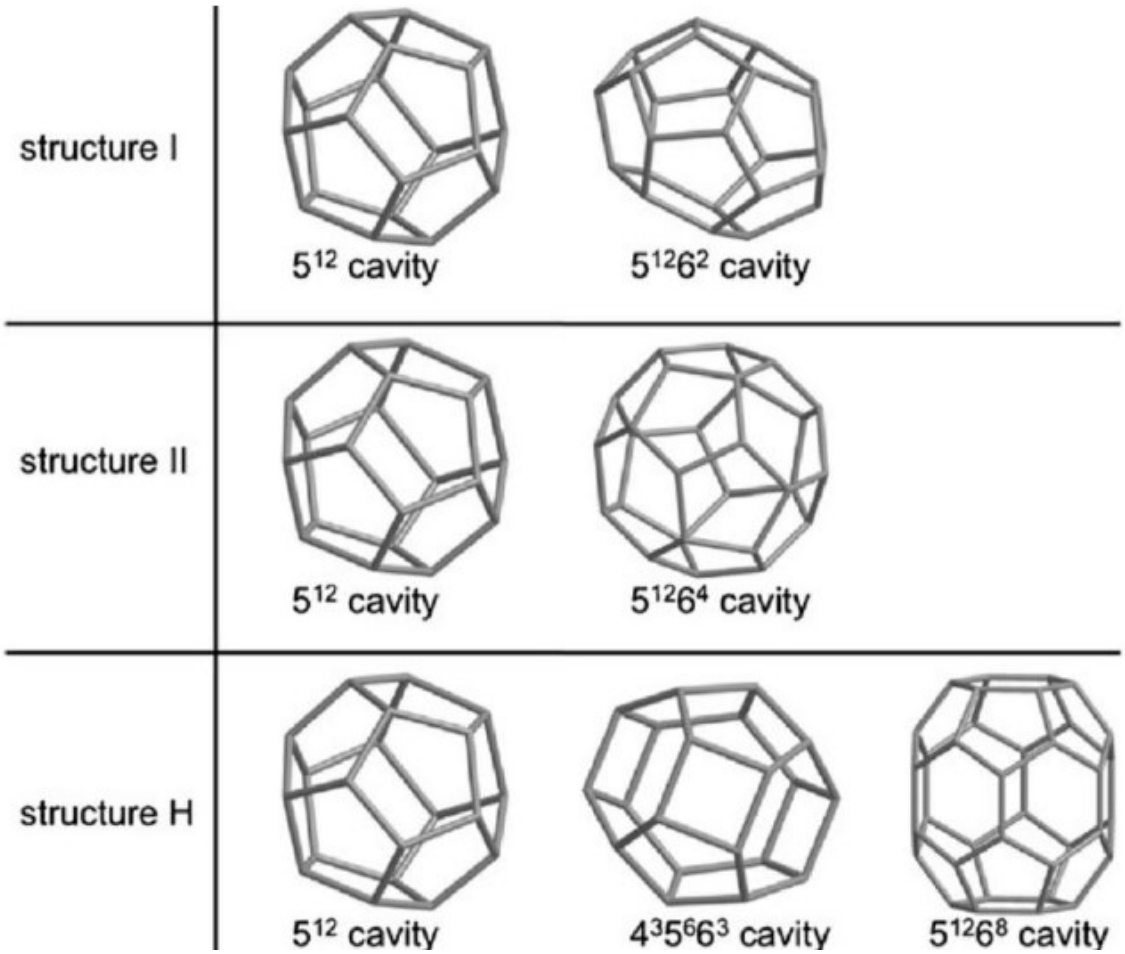

Figure 1.1: The three types of clathrate structures. Structure I hold smaller molecules, mostly methane and carbon dioxide. Structures II and H store larger hydrocarbons (Aresta et al., 2015).

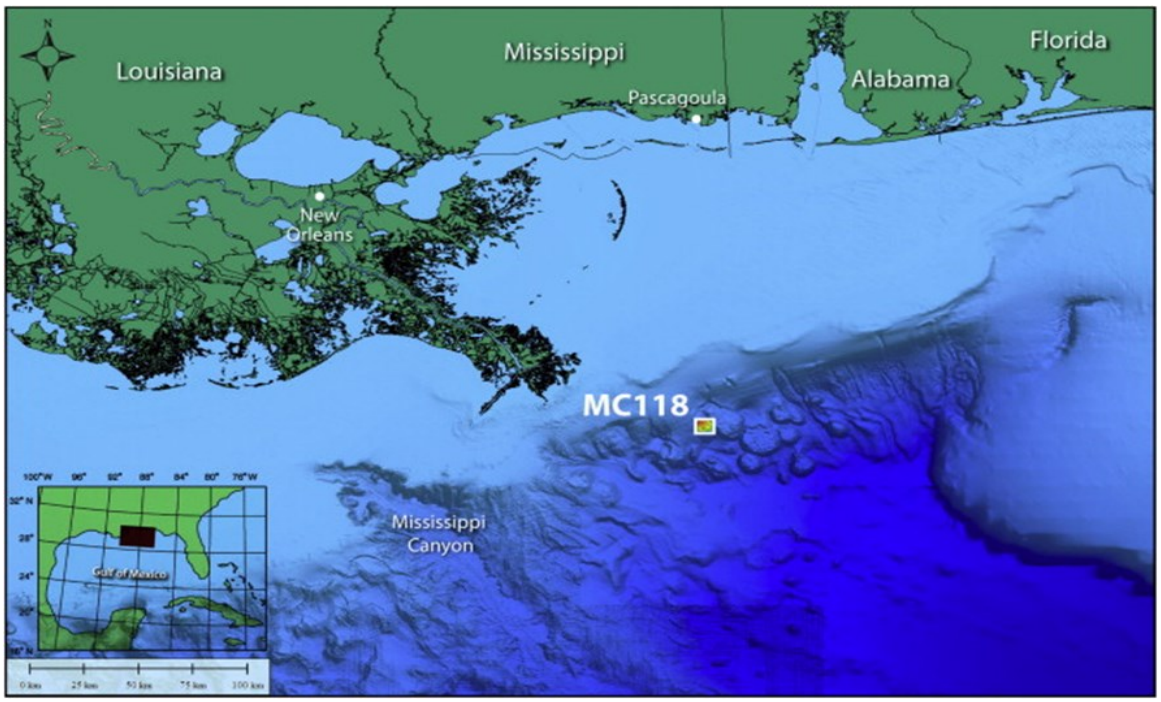

Figure 1.2: MC118, located in the Northern Gulf of Mexico. Resting on the continental slope, it's appropriately positioned for the formation of gas hydrates (Simonetti et al., 2013)

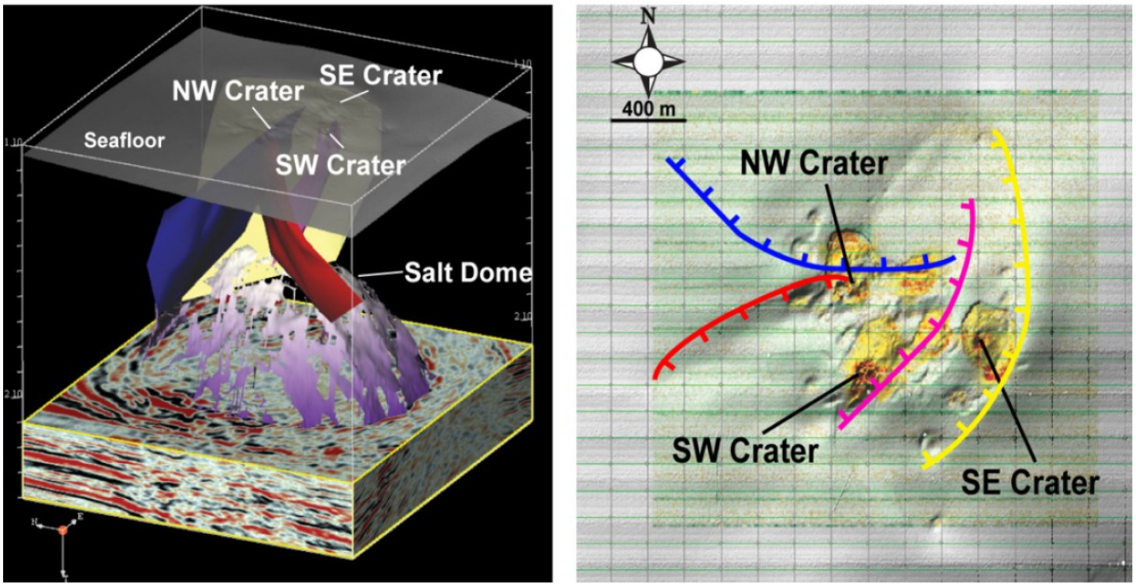

Figure 1.3: A) Shows the interpreted location of the salt dome located within the seismic section and main associated faults underneath Woosley Mound at MC-118; B) An aerial view of Woolsey Mound and the faults as they intersect the seafloor (Macelloni et al., 2012).

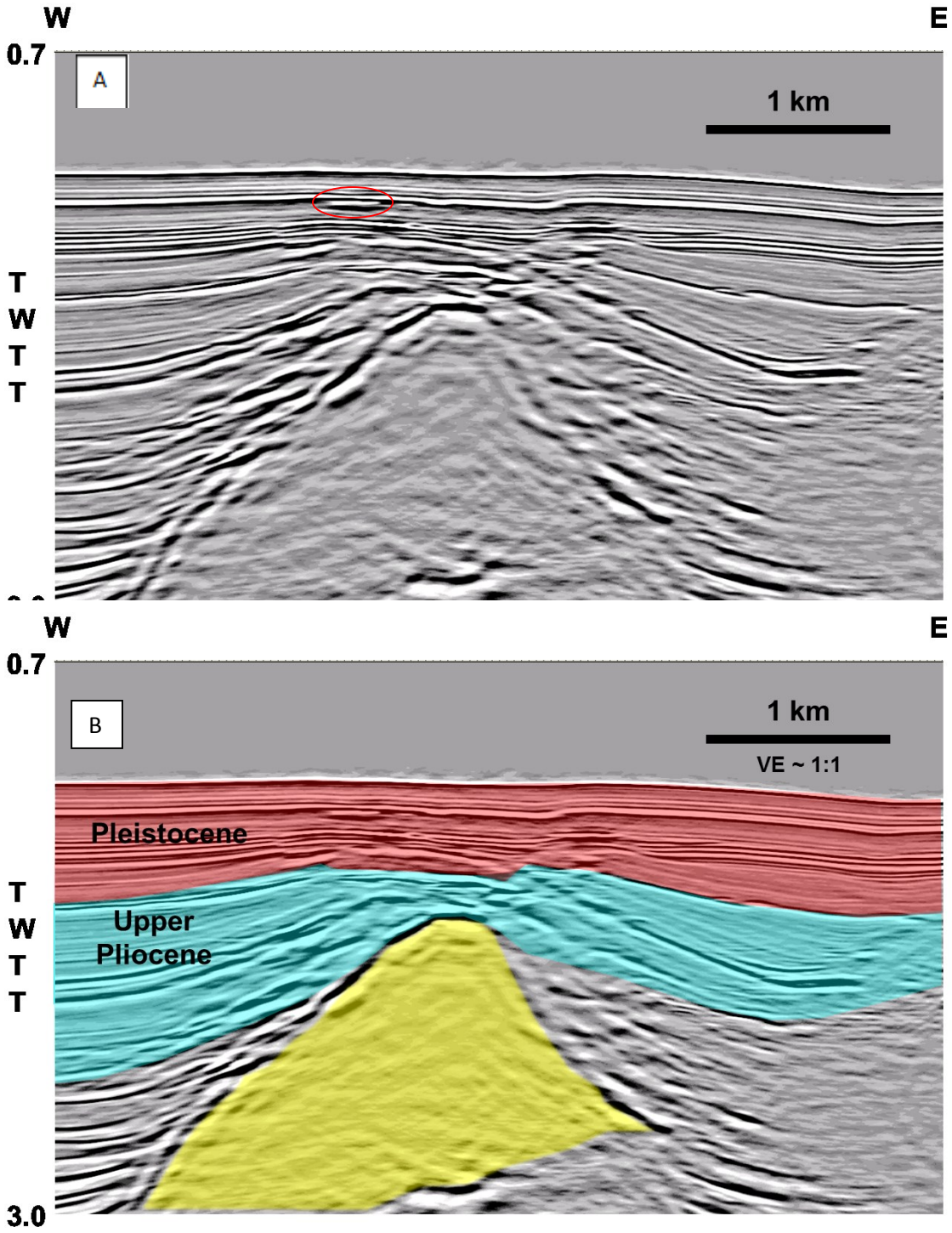

Figure 1.4: A) Uninterpreted seismic profile at MC-118. The red circle indicates the high amplitude negative reflector associated with the BGHSZ described in Simonetti et al. (2013); B) Seismic profile at MC-118 showing the interpreted location of the salt in yellow highlighted (Knapp, J.H., unpublished)

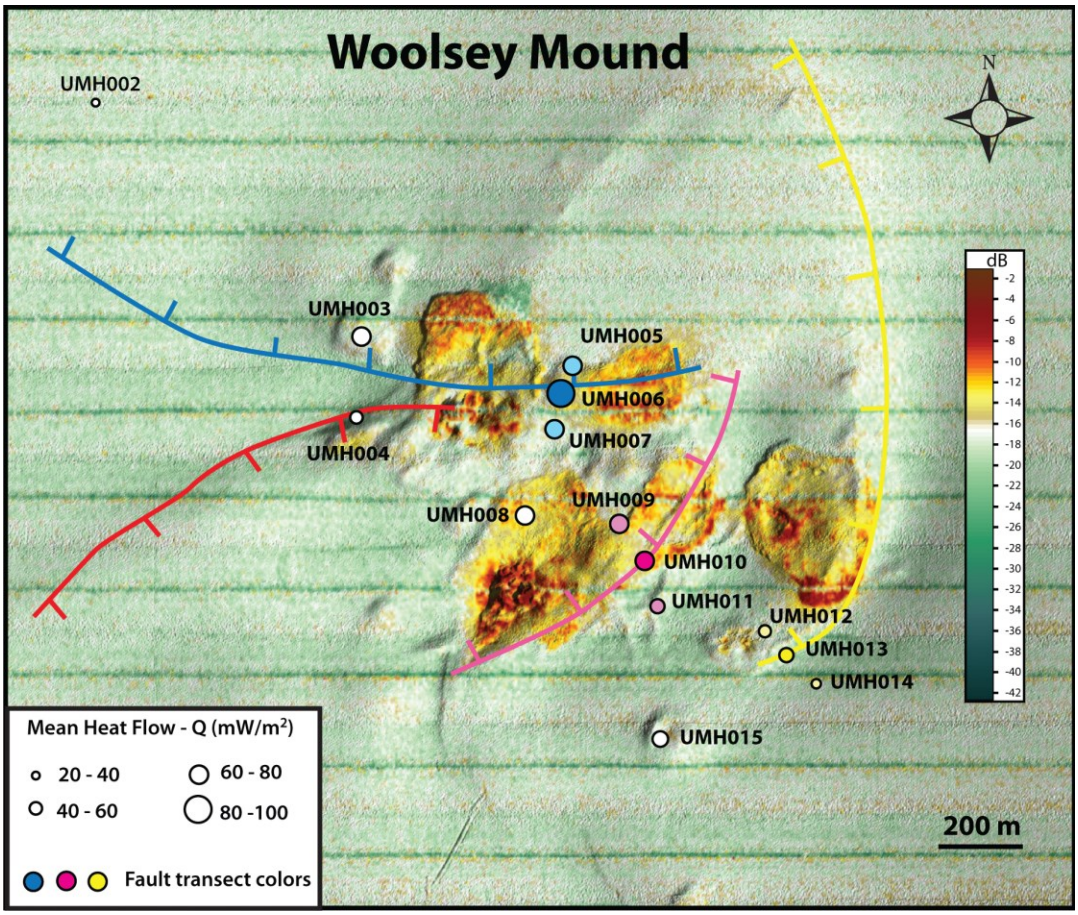

Figure 1.5: Map of the heat flow measurement locations, taken in transects along major faults, pockmarks, and at a reference point away from the salt diapir. The higher heat flow values are indicated but the larger cirlces, and are associated with the intersection of the faults with the seafloor. This indicates that the faults are migration pathways for heat. (Macelloni et al., 2015)

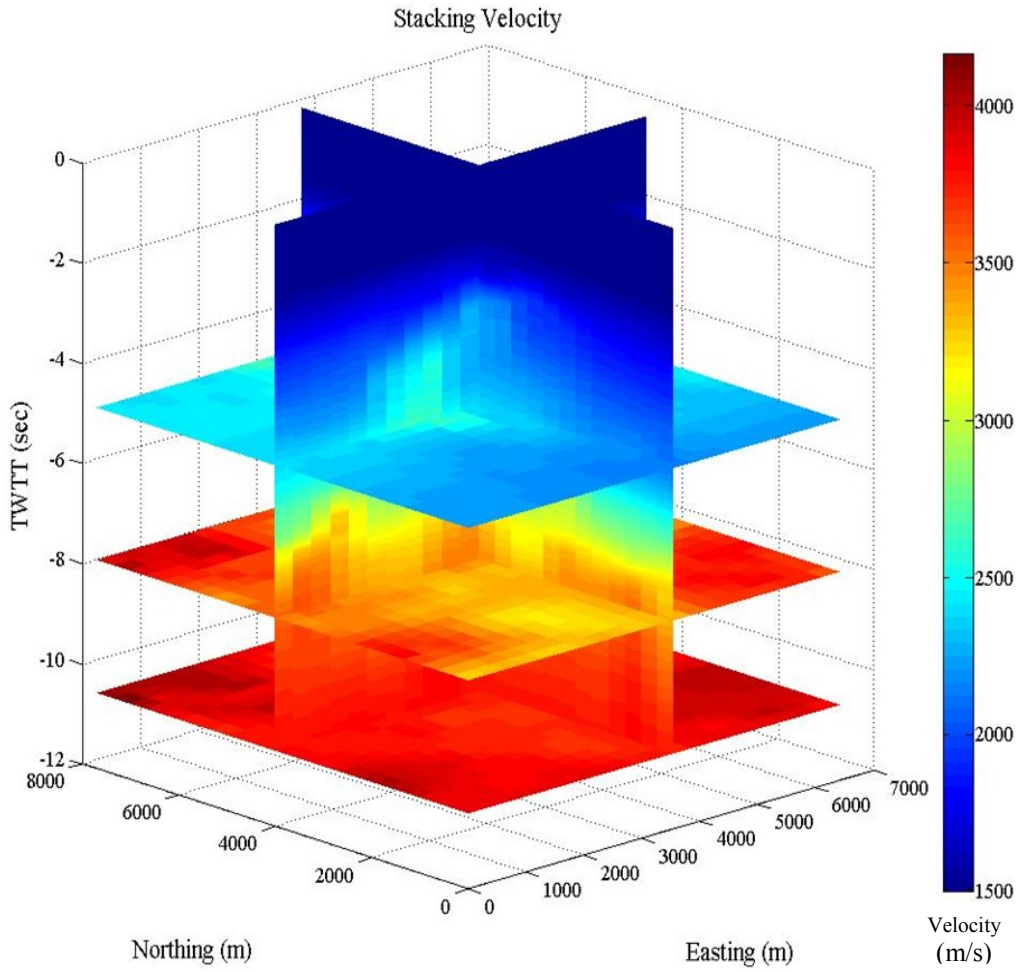

Figure 1.6: 3D stacking velocities (in m/s) from the WesternGeco dataset. The x and y axes show locations in meters and the z axis displays two way travel time. The scale shows velocity where blue is slower, and read is higher velocity. The data shows an overall increase in velocity with depth.

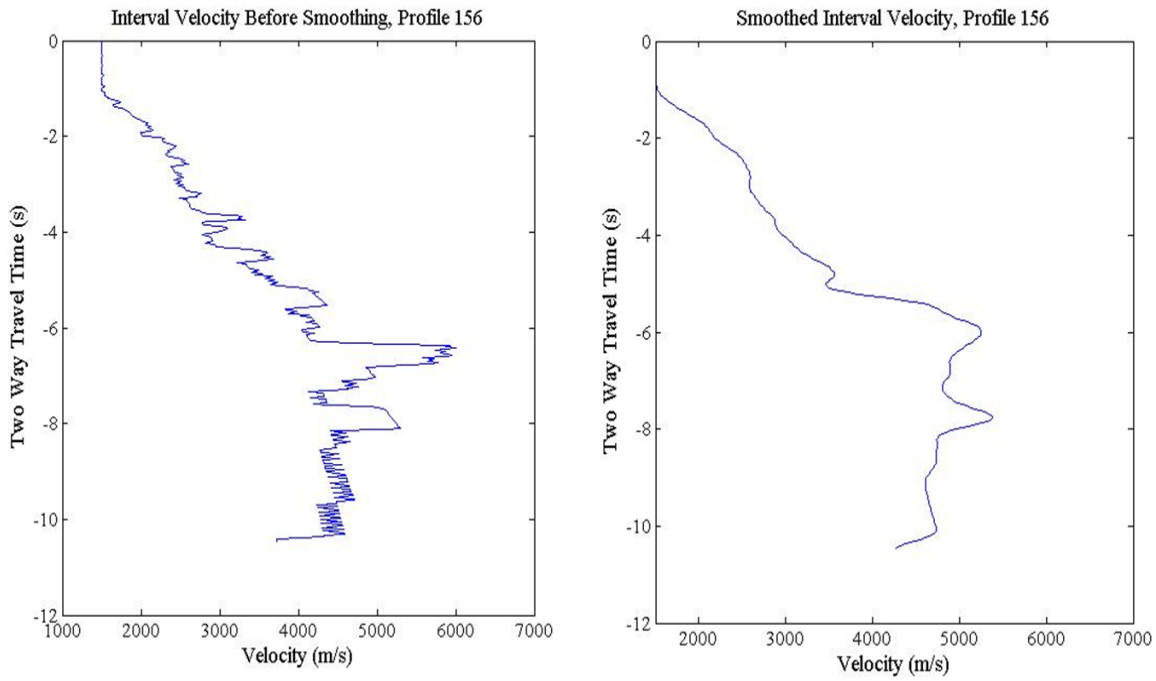

Figure 7: A) Interval velocity profile (in m/s) for one depth point without smoothing the errors associated with converting from stacking velocity using Dix equation. B) Smoothed interval velocity using a box filter.

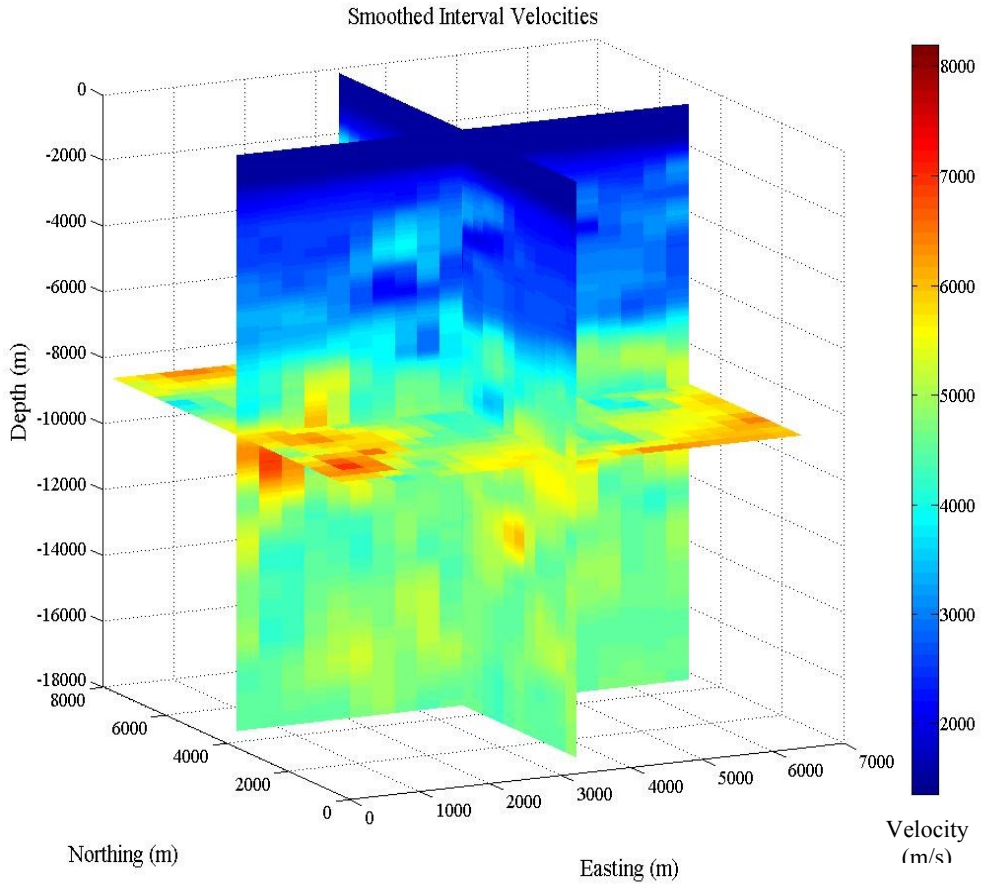

Figure 1.8: 3D display of the smoothed interval velocities (in m/s) used in converting the location of the top of the salt.

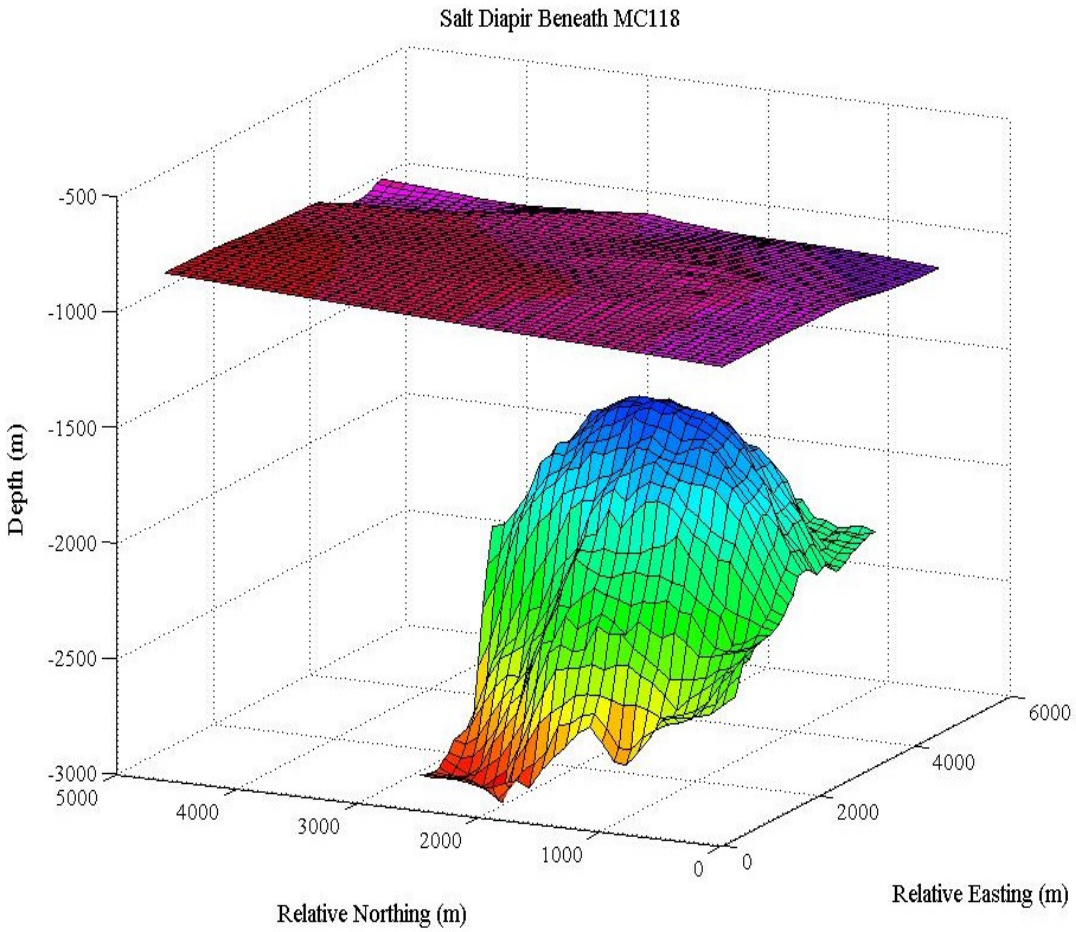

Figure 1.9: Interpolated locations of the salt beneath the topography of MC118 based on the seismic, and converted to depth using the velocities. The top layer of topography shows depth beneath the sea surface.

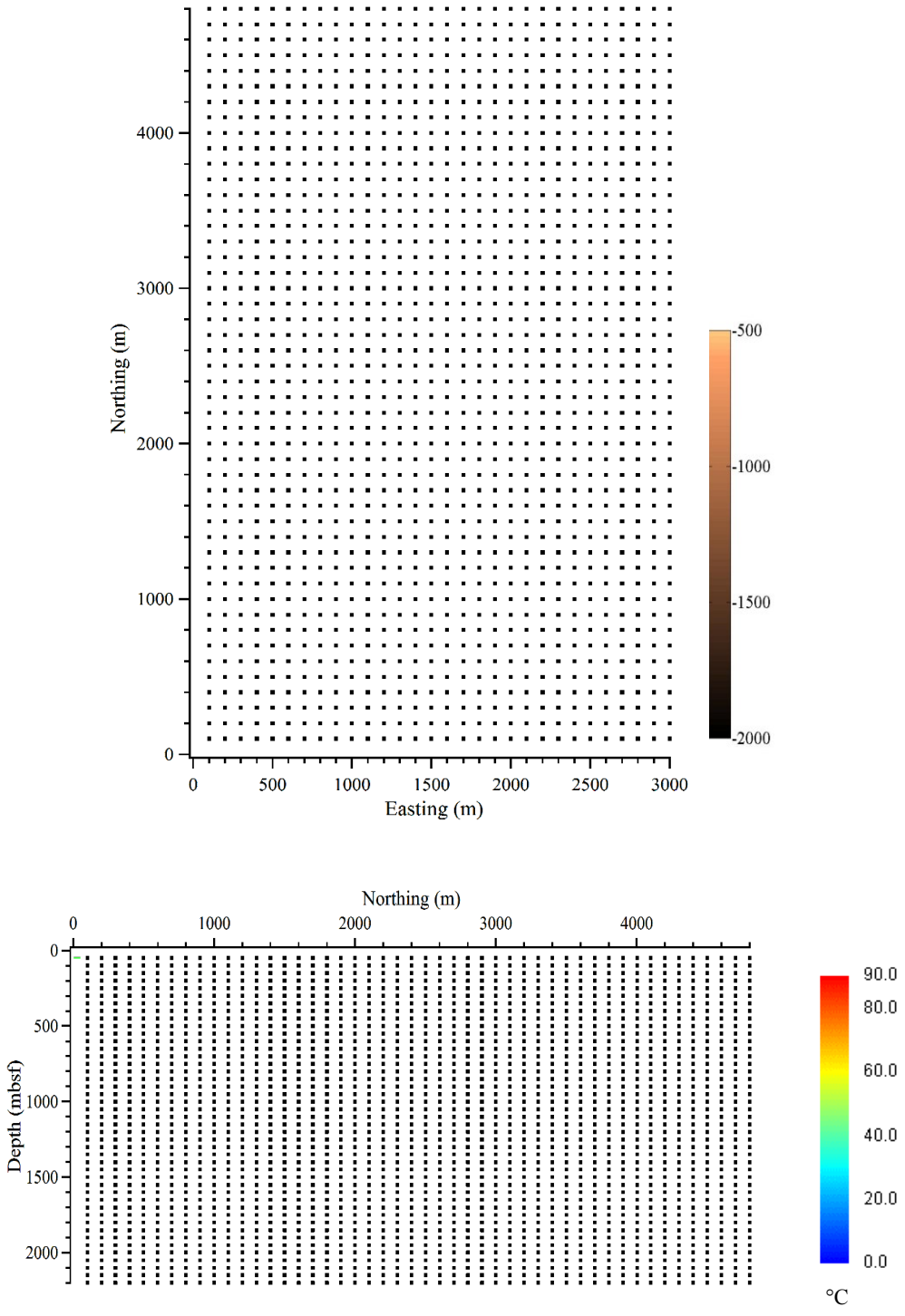

Figure 1.10: A) Aerial extent of the area covered by the thermal model with a plot of where the salt is located and the contoured depth at which it is located; B) 2D Profile of the thermal model set at initial conditions, prior to running the thermobaric model.

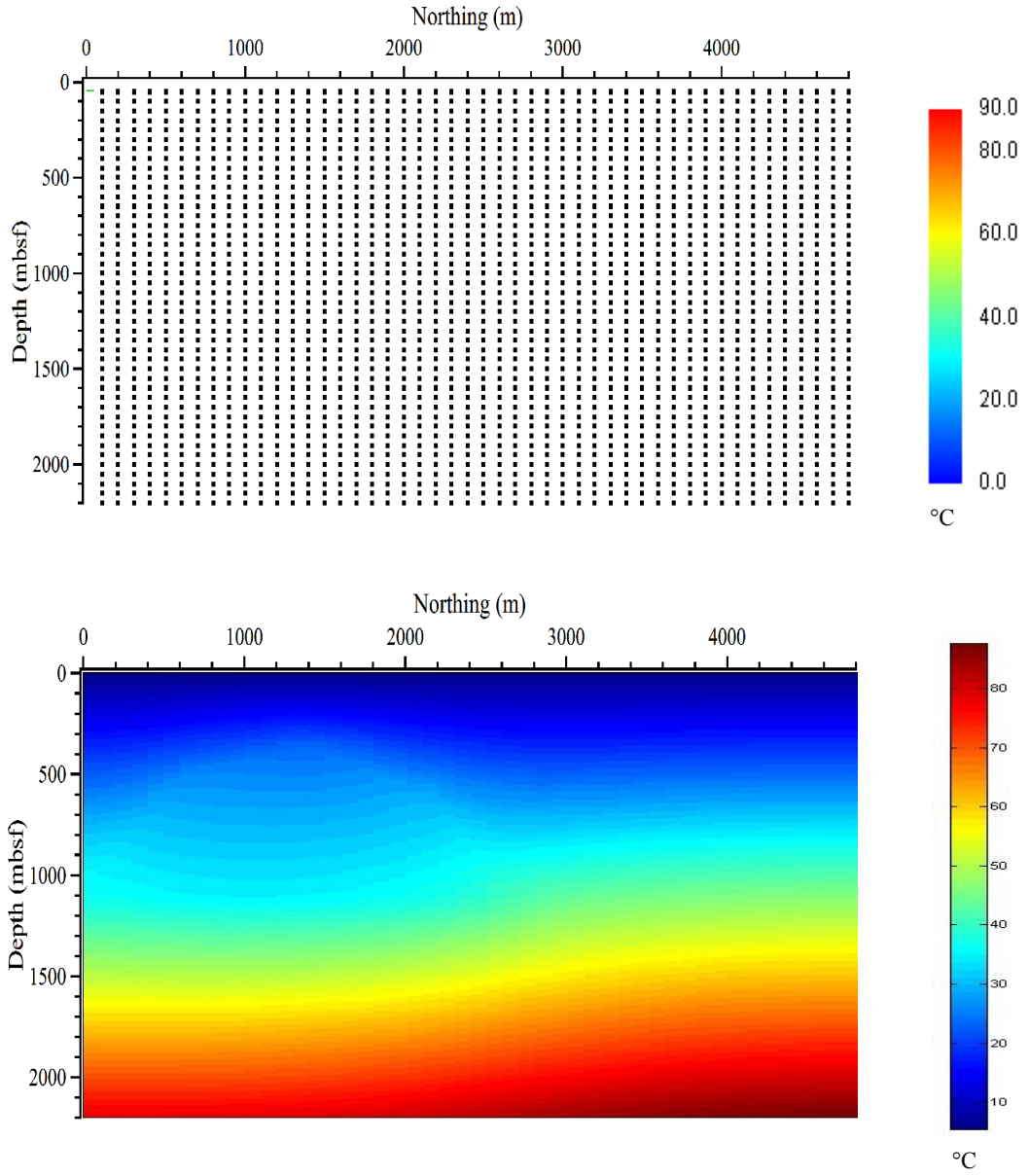

Figure 1.11: Both plots show the finial temperature output of the HYDROTHERM model over the shallowest part of the salt dome. The y-axis shows depth, down to 2,400m and the x-axis shows relative northing, where the northern most position is the right side of the plot. The dome shape appearance in the temperature profile is associated with the presence of salt, creating a thermal high. A) 2D temperature model (in °C) with nodes of temperature after running the code to steady state conditions. B) Temperatures imported into Matlab without the nodes.

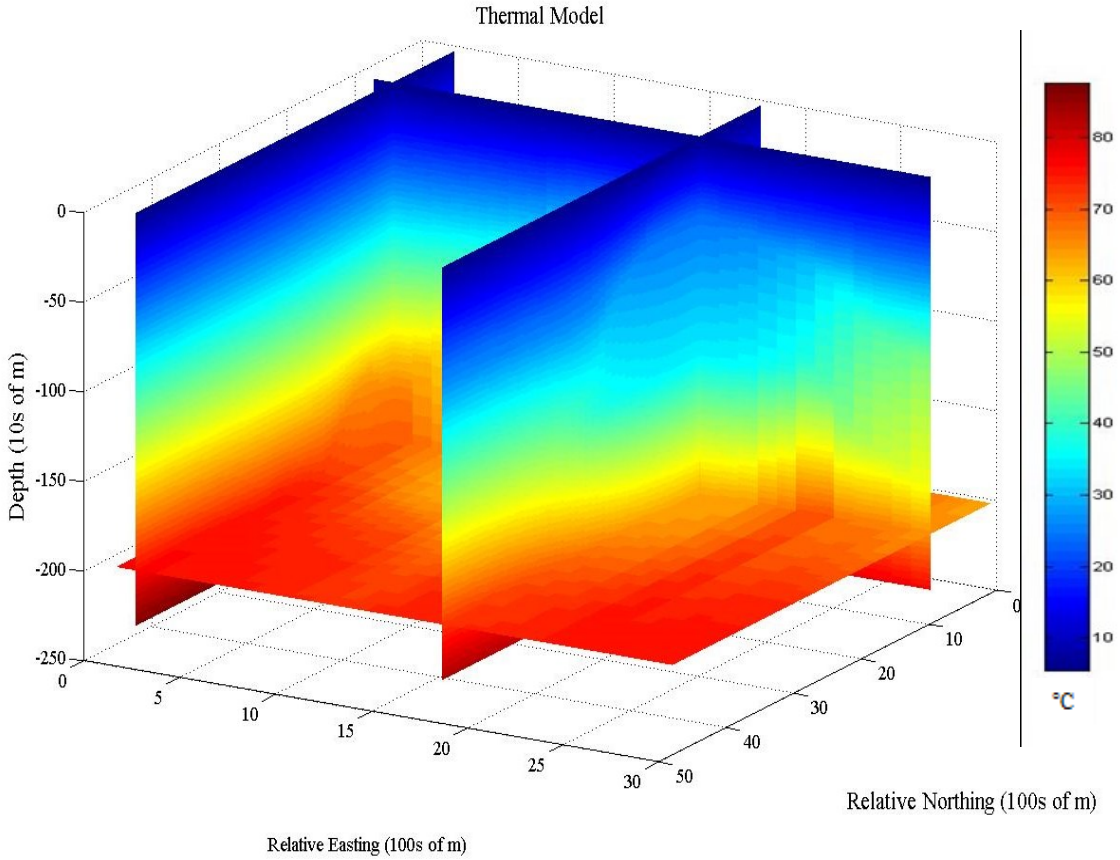

Figure 1.12: Pseudo 3D temperature plot with cooler temperatures represented by the blue color, and warmer colors increasing up the color bar to red, which is the warmest temperatures. The salt diapir is clearly delineated by the dome shape of increase temperatures in the profile along Relative Easting line 17 (the right most profile). The lack of salt creates a regular temperature distribution as seen in the profile furthest to the left, Relative Eating line 2.

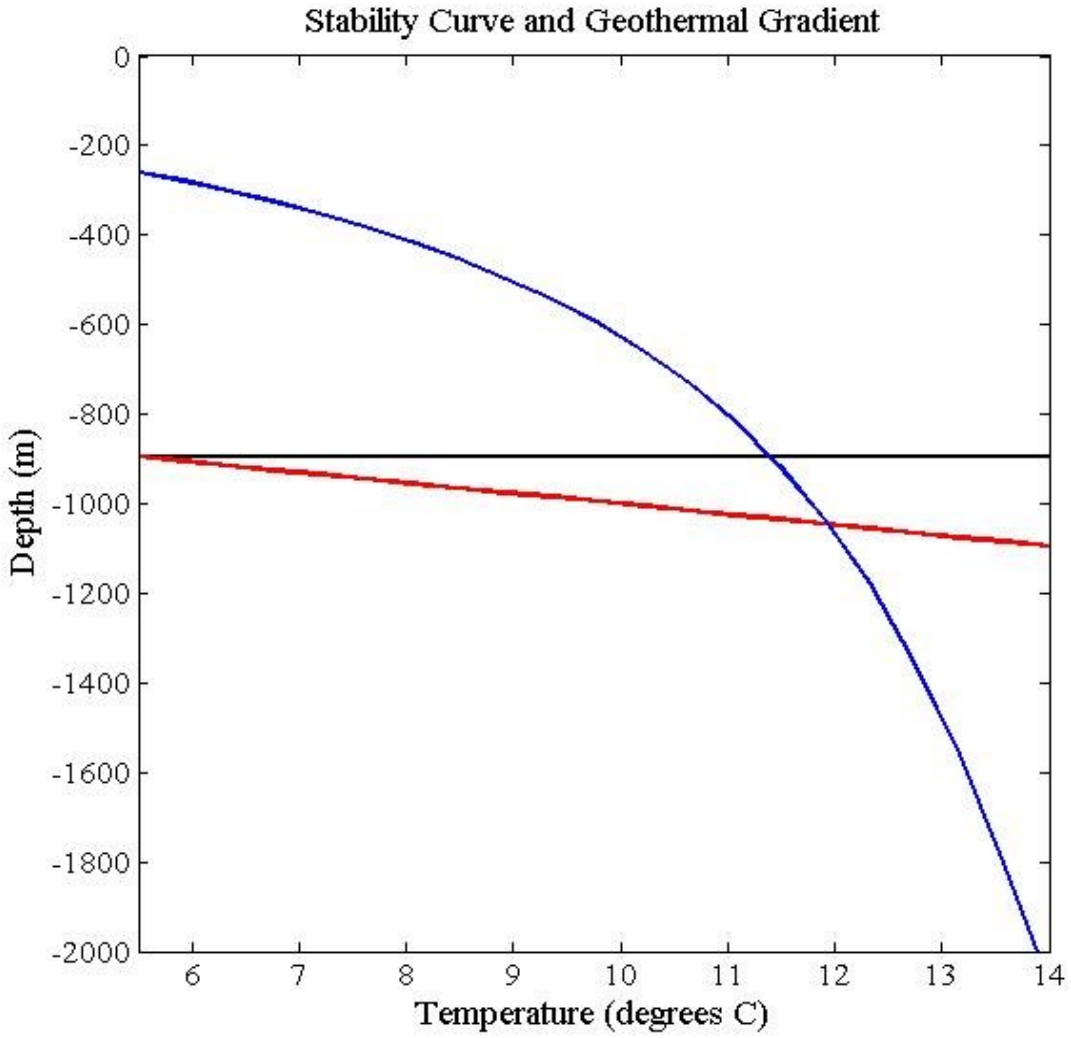

Figure 1.13: Thermobaric stability plot for one of 810 locations calculated. The blue line represents the stability curve of the gas hydrate, the black line is the depth of the sea floor below sea level, and the red line is the geothermal gradient, 31 ^{0}C/km, which was taken directly from the temperature measurements calculated using HYDROTHERM.. The intersection of the stability curve and the geothermal gradient (blue and red lines respectively) is the lowest depth within the subsurface that the gas hydrates will be stable. This is based on a seafloor temperature of 5.5 ^{0}, and a gas composition of 92.2% methane, 6.4% ethane, and 1.1% propane, based after Macelloni et al. (2015).

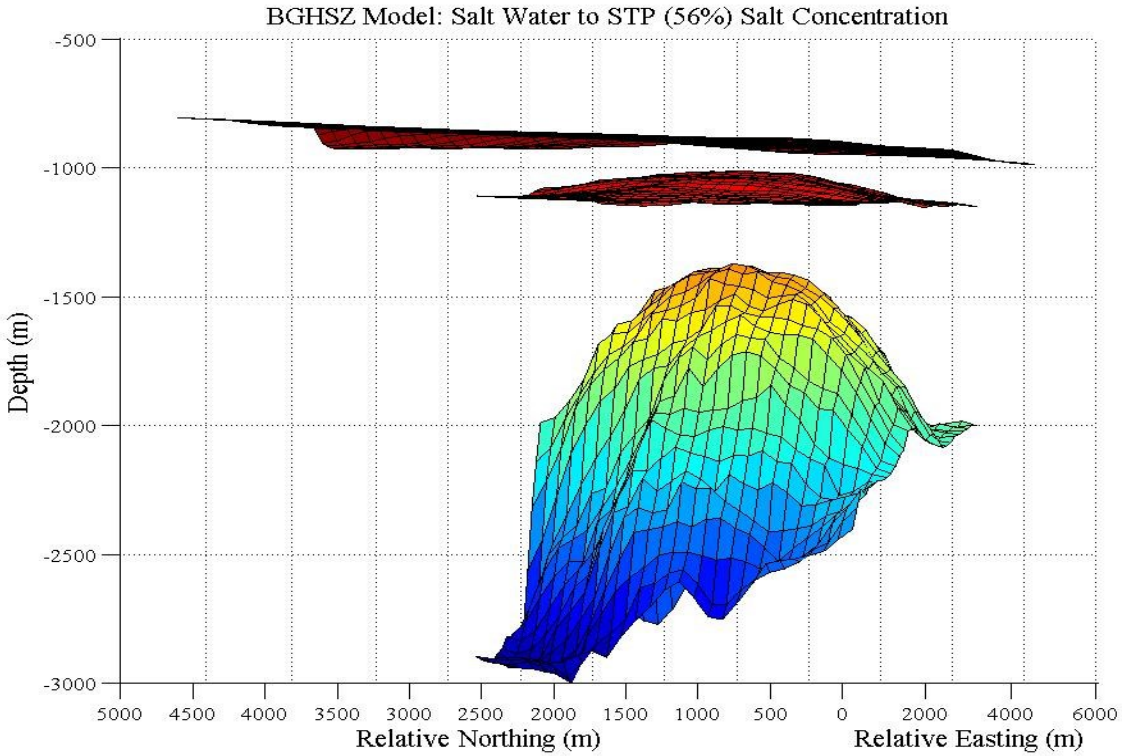

Figure 1.14: Map of the BGHSZ located beneath the mapped seafloor and above the salt diapir with a varying salt concentration ranging from sea water levels to standard temperature and pressure condition. The coloring of the layers is only shown to give perspective on the change in depth between the layers. The 3D image has been rotated to show a side view of the dome in relation to the topography and BGHSZ so the thickness of the stability zone below seafloor can be displayed

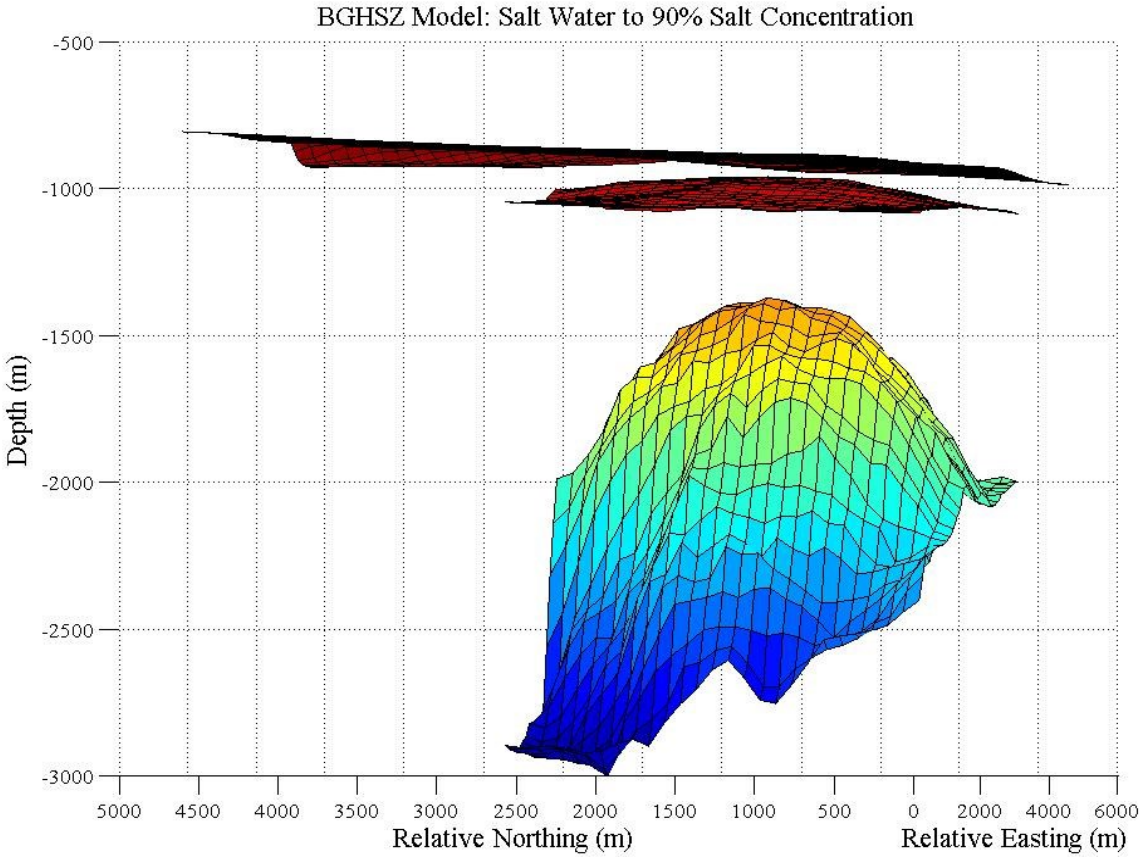

Figure 1.15: Map of the BGHSZ located beneath the mapped seafloor and above the salt diapir with a varying salt concentration from sea water levels to 90 weight percent salt. The coloring of the layers is only shown to give perspective on the change in depth between the layers. The 3D image has been rotated to show a side view of the dome in relation to the topography and BGHSZ so the thickness of the stability zone below seafloor can be displayed

REFERENCES

Aresta, Michele; Dibenedetto, Angela; Quaranta, Eugenio (Eds.) 2015. Thermodynamics and Applications of CO2 Hydrates. In, *Reaction Mechanisms in Carbon Dioxide Conversion*, Springer, pp.373-402

Buffet, Bruce A., 2000, Clathrate Hydrates, Earth Plant. Science, pg. 447-507

Collett, T., Lee, M., Lewis, R., Mrozewski, S., Guerin, G., Goldberg, D., Cook, A., 2012. Gulf of Mexico gas hydrate joint industry project leg II logging-while-drilling data acquisition and analysis. J. Mar. Petrol. Geol. 34, 41e61.

Helgerud, M.B., Dvorkin, J., Nur, A., Sakai, A., Collett, T., 1999. Effective wave velocity in marine sediments with gas hydrates: effective medium modeling. Geophys. Res. Lett. 26, 2021e2024

Husson L., Le Pichon X, Henry P. Flotte N. &. Rangin C.(2008). – Thermal regime of the NW shelf of the Gulf of Mexico. Part B) Heat Flow. – Bull. Soc. géol. Fr., 179, 2, 139-145

Hyndman, R.D., Spence, G.D., 1992. A seismic study of methane hydrate marine bottom simulating reflectors. J. Geophys. Res. 97, 6683e6698. http://dx.doi.org/10.1029/92JB00234.

Jamshidzadeh, Z; Tsai, F.T.C.; Ghasemzadeh, H; Mirbagheri, S.A.; Barzi, M.T.; Hanor, J.S. 2015. Dispersive Thermohaline Convection Near Salt Domes: a Case at Napoleonville Dome, Southeast Louisiana, USA. Springer. Hydrogeology Journal. 23:983-998

Kipp, K.L., Jr., Hsieh, P.A., and Charlton, S.R., 2008, Guide to the revised ground-water flow and heat transport simulator : HYDROTHERM — Version 3: U.S. Geological Survey Techniques and Methods 6−A25, 160 p.

Kvenvolden, K.A., Ginsberg, G.D., Soloviev, V.A., 1993. Worldwide distribution of subaquatic gas hydrates. Geo-Marine Lett. 13 (1), 32e40.

Lapham, L.L., Chanton, J.P., Martens, C.S., Woolsey, J.R., 2008. Microbial activity in surficial sediments overlying acoustic wipe-out zones at a Gulf of Mexico cold seep. Geochem. Geophys. Geosyst. 9 (6).

Liu, X., Fleming, P.B., 2007. Dynamic multiphase flow model of hydrate format marine sediments. J. Geophys. Res. 112 (B03101), 1e23.

Macelloni, L., Simonetti, A., Knapp, J.H., Knapp, C.C., Lutken, C.B., Lapham, L., 2012. Multiple resolution seismic imaging of a shallow hydrocarbon plumbing system,Woolsey Mound, Northern Gulf of Mexico. Journal of Marine and Petroleum Geology 38, 128e142.

Macelloni, L, Lutken, C.B, Garg, S., Simonetti, A., D'Emidio, M., Wilson, R.M., Sleeper, K., Lapham, L., Lewis, t., Pizzi, M., Knapp, J., Knapp, C., and McGee T.M., 2015, Heat-Flow Regimes and the Hydrate Stability Zone of a Transient, Thermogenic, Fault-Controlled Hydrate System (Woolsey Mound Northern Gulf of Mexico). Marine and Petroleum Geology. Vol. 59, 491-504

Ruppel, C., Dickens, G.R., Castellini, D.G., Gilhooly, W., and Lizarralde, D., 2005, Heat and salt inhibition of gas hydrate formation in the northern Gulf of Mexico, Geophysical Research Letters, vol. 32, LO46605.

Salvador, A., 1987. Late Triassic-Jurassic paleogeography and the origin of the Gulf of Mexico. AAPG Bulletin, v.71, p.419-451.

Sassen, R., Roberts, H.H., Jung, W., Lutken, C.B., DeFreitas, D.A., Sweet, S.T., Guinasso Jr., N.L., 2006. The Mississippi Canyon 118 Gas Hydrate Site: a Complex Natural System: OTC Paper #18132. Offshore Technology Conference, Houston,TX.

Simonetti, A., Knapp, J. H., Knapp, C. C., Macelloni, L., Lutken, C. B., 2011, Defining the hydrocarbon leakage zone and the possible accumulation model for marine gas hydrates in a salt tectonic driven cold seep: examples from Woolsey Mound, MC118, northern Gulf of Mexico, Proceedings of the 7th International Conference on Gas Hydrates (ICGH 2011), Edinburgh, Scotland, United Kingdom, July 17-21, 2011.

Simonetti, A., Knapp, J.H., Sleeper, K., Lutken, C.B., Macelloni, L., Knapp, C.C., 2013. Spatial distribution of gas hydrates from high-resolution seismic and core data, Woolsey Mound, Gulf of Mexico. J. Mar. Petrol. Geol. 44, 21e33.

Singh, S.C., Minshull, T.A., Spence, G.D., 1993. Velocity structure of a gas hydrate reflector. Science 260, 204e207.

Shedd,W., Boswell, R., Frye, M., Godfriaux, P., Kramer, K., 2011. Occurrence and nature of “bottom simulating reflectors” in the northern Gulf of Mexico. Journal of Marine and Petroleum Geology.

Shipley, T.H., M.H. Houston, R.T. Buffler, F.J. Shaub, K.L. McMillen, J.W. Ladd & J.L. Worzel, 1979, Seismic evidence for widespread possible gas hydrate horizons on continental slopes and rises: AAPG Bulletin63, 2204-2213

Sloan, E.D., 1990, Clathrate Hydrates of Natural Gas, Marcel Decker Inc, Publishers, New York

Sloan, E.D., 1998, Clathrate Hydrates of Natural Gas, 2nd ed. Marcel Decker Inc, Publishers, New York

Sloan, E.,D., Koh, C., 2008. Clathrate Hydrates of Natural Gases, third ed. CRC Press., p. 721

Smith, A.J., Flemings, P.B., Fulton, P.M., 2014. Hydrocarbon flux from natural deepwater Gulf of Mexico vents. Earth Planet. Sci. Lett. 395, 241e253.

U.S. Department of State (2007). Projected Greenhouse Gas Emissions. In: Fourth Climate Action Report to the UN Framework Convention on Climate Change c. U.S. Department of State, Washington, DC, USA.

U.S Nuclear Regulatory Commision. Survey of Salt Dome Investigations. By Peter Hart, Robert L. Johnson, Thomas J. Nicholson, Ellen Quinn, and Robert J. Wright. N.p.: n.p., 1981. Print.

Van der Waals, J.H. and Platteeuw, J.C. 1959. Clathrate Solutions. Advances in Chemical Physics. Vol. 2, 1-57

Wu, Shengyu; Bally, Albert W.; Cramex, Carlos 1990. Allochthonous salt, structure and stratigraphy of the north-eastern Gulf of Mexico. Part II Structure. Marine and Petroleun Geology 7(4):318-3